Fracture Mechanics of Concrete and Concrete Structures - Assessment, Durability, Monitoring and Retrofitting of Concrete Structures- B. H. Oh, et al. (eds)

Modeling formation of cracks in concrete cover due to reinforcement corrosion

A. Michel, M. R. Geiker, H. Stang & J. F. Olesen
Department of Civil Engineering, Technical University of Denmark

A. O. S. Solgaard
COWI A/S & Department of Civil Engineering, Technical University of Denmark

ABSTRACT: An electrochemical and mechanical modeling approach to simulate formation of corrosion induced cracks in reinforced concrete structures is presented. The electrochemical model allows simulation of the propagation of macro cell corrosion in a homogeneous defect-free concrete-steel system. To simulate cracking a finite element based crack propagation model is proposed. To demonstrate the potential use of the combined modeling approach a numerical example is provided where the influence of various exposure conditions on the corrosion current density and subsequent formation of cracks is illustrated.

1 INTRODUCTION

One of the major deterioration problems of reinforced concrete structures is corrosion of steel causing considerable damages and costs due to maintenance and repair needs. In Europe more than € 250 billion are spent annually for maintenance and repair of concrete structures due to deterioration (Li (2004)), in which corrosion of reinforcing steel is estimated to be related to 90% of the degradation problems (Rendell et al. (2002)). Corrosion can cause formation of cracks in the concrete cover as well as cross sectional reduction of reinforcement area affecting strength and serviceability of reinforced concrete structures. Prediction of the corrosion process as well as the subsequent formation and propagation of cracks could be used for prediction of residual service life and support maintenance planning of reinforced concrete structures.

A variety of models dealing with corrosion induced concrete cover cracking can be found in the literature. The available models can be broadly divided into empirical, e.g. Alonso et al. (1998), analytical, e.g. Bazant (1979), Chernin et al. (2009), and numerical models, e.g. Molina et al (1993). Some of the models include various phenomena associated with corrosion induced cover cracking, such as diffusion of corrosion products, e.g. Liu & Weyers (1998) and debonding, e.g. Noghabai (1999). Most of the models show reasonable agreement with experimental results obtained from accelerated corrosion tests, e.g. Andrade et al. (1993), Val et al. (2009). However, the use of the models to predict corrosion induced cover cracking is limited since a constant corrosion rate is assumed, which is unlikely for concrete structures subjected to realistic exposure conditions.

In the present paper the theoretical framework for a combined modeling approach is presented, which allows prediction of the corrosion rate of steel in concrete and the resulting formation of cracks in the concrete cover. The formation of $Fe_2O_3 \cdot H_2O$ as uniformly distributed corrosion products is assumed (see e.g. Marcotte & Hansson (2007), Küter (2009)). In contrast to previously presented models, the proposed electrochemical and mechanical modeling approach does not assume a constant corrosion rate of the reinforcement. An electrochemical corrosion model is used to predict the corrosion rate of the reinforcement accounting for the impact of varying exposure conditions. Focus is placed on the propagation stage of macro cell corrosion with prescribed anodic and cathodic reinforcement regions. Application of Faraday´s law allows to link the FEM based corrosion model with a crack propagation model by determining the rate of formation of corrosion products from predicted corrosion current densities. To model the corrosion induced cracks in the concrete cover, a FEM based crack model is proposed. The developed model focuses on the propagation of cracks in the concrete cover. Cracking of the concrete is described by a cohesive discrete cracking approach with a multilinear softening cohesive relation. The expansive nature of the corrosion products is modeled using a thermal analogy. The assumptions made in the present study allow a conservative prediction of

the corrosion rate of reinforcement and the subsequent corrosion induced concrete cover cracking.

Finally, a numerical example is given illustrating the potential use of the proposed modeling approach taking into account the impact of various exposure conditions on the corrosion rate of steel and the corrosion induced cover cracking.

2 MODELLING APPROACH

2.1 *Two-phase FEM based corrosion model*

To model the corrosion process of reinforcement in concrete structures a physio-chemical, FEM based corrosion model has been established. In the model electrochemical corrosion processes are combined with transport mechanisms to allow simulation of the propagation of macro cell corrosion in a homogeneous defect-free concrete-steel system. The system modeled is illustrated in Figure 1. Since the proposed corrosion model is dealing with the propagation stage of reinforcement corrosion the anodic and cathodic areas of the reinforcement are prescribed.

For the description of the electrochemical processes in the concrete pore solution acting as electrolyte two physical laws can be used (see e.g. Warkus et al. (2006)). The first one is Laplace's equation, which describes the potential distribution in the concrete pore solution assuming electrical charge conservation and isotropic conductivity

$$\nabla^2 \phi = 0 \tag{1}$$

where ∇ = nabla operator and ϕ = potential. The second is Ohm´s law describing the rate of dissolution of iron on the steel surface in concrete if the potential distribution and the resistivity of the electrolyte are known (Isgor & Razaqpur (2006))

$$i = -\frac{1}{\rho_T}\frac{\partial \phi}{\partial n} \tag{2}$$

where i = current density, ρ_T = concrete resistivity and n = direction normal to the rebar surface.

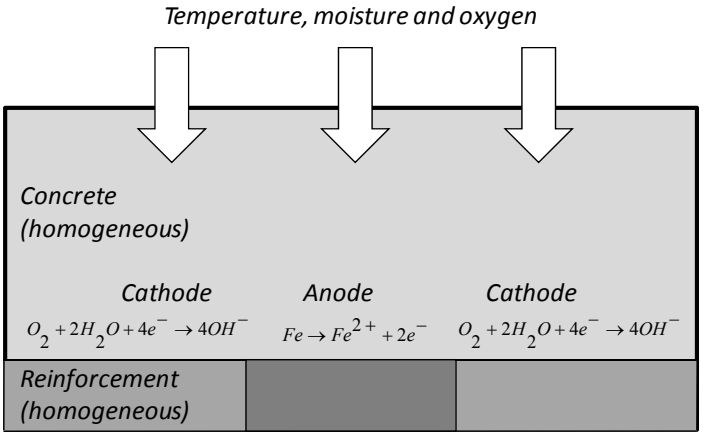

Figure 1. Two-phase FEM based corrosion model.

In order to solve Laplace´s equation (Eq. 1) appropriate boundary conditions are needed in the form of so-called polarization or potential-current curves quantifying the relation between current and potential at the steel surface. For the anodic and cathodic regions of the steel surface the boundary conditions can be defined as

$$\phi = \phi_A \quad \text{and} \quad \phi = \phi_C \tag{3}$$

where ϕ_A = anodic potential and ϕ_C = cathodic potential. Assuming that the steel surface polarizes due to activation and concentration polarization, the boundary conditions for the anodic and cathodic regions of the steel can be expressed as follows

$$i_A = i_{0,A}\alpha_A$$
$$\text{with} \quad \alpha_A = \exp\left(\ln 10 \frac{\phi_A - E_{0,A}}{b_A}\right) \tag{4}$$

where i_A = anodic current density, $i_{0,A}$ = anodic exchange current density, $E_{0,A}$ = anodic equilibrium potential and b_A = anodic Tafel constant and

$$i_C = i_{0,C}\frac{1-\alpha_C}{1+\frac{i_{0,C}}{i_{Lim}}\alpha_C}$$
$$\text{with} \quad \alpha_C = \exp\left(-\ln 10 \frac{\phi_C - E_{0,C}}{b_C}\right) \tag{5}$$

where i_C = cathodic current density, $i_{0,C}$ = cathodic exchange current density, $E_{0,C}$ = cathodic equilibrium potential, b_C = cathodic Tafel constant and i_{Lim} = limiting current density. More information on the theory of polarization phenomena of metals in an electrolyte can be found e.g. in Stern & Geary (1957), Bardal (2004).

Potential distribution in the concrete pore solution and hence the corrosion rate of the reinforcement (see Eq. 2) are strongly influenced by exposure conditions as well as material properties of the reinforced concrete structure. To account for the impact of environmental conditions and material properties on the polarization behavior of the steel surface a set of partial differential equations (PDE's) is solved. In particular the distribution of temperature, moisture, oxygen and resistivity in the concrete domain and along the concrete-steel interface are of interest.

Distribution of a potential, such as temperature, moisture and oxygen gradients, as well as the corrosion process itself in concrete and along the concrete-steel interface can be described by a quasi-harmonic equation of the form (Isgor & Razaqpur (2006))

$$\alpha \frac{\partial X}{\partial t} + \nabla\left(D_X \nabla X\right) + Q = 0 \tag{6}$$

where α = coefficient representing material properties, X = potential, t = time, D_X = corresponding transport functions for potential X and Q = sink term for negative values and a source term for positive values.

The time dependent moisture distribution in the concrete domain is determined by solving Equation (6) with a moisture dependent transport coefficient as corresponding transport function for the moisture potential. A number of empirical and analytical expressions for the moisture dependent transport coefficient can be found in the literature e.g. in Künzel (1994), Bazant (1994) and Pel (1995). In the present study an exponential function for the moisture dependent transport coefficient proposed by Wittmann (1992) is selected to describe the moisture transport in concrete

$$D_{RH} = a + b\exp\left(RHc\right) \tag{7}$$

where D_{RH} = moisture transport function, a,b,c = non-physical fitting parameters and RH = relative humidity. It should be noted that effects of hysteresis (see e.g. Scheffler (2009)) are not taken into account in the present modeling approach. However, to demonstrate the potential use of the proposed combined modeling approach to predict the corrosion rate as well as propagation of cracks in the cover of reinforced concrete structures such a simplification seems to be appropriate.

The limiting current density term, i_{Lim}, introduced in Equation (5) describing the polarization of cathodic reinforcement sites indicates that oxygen availability plays an important role in the polarization behavior. A function for i_{Lim} can be obtained combining Faraday´s law with Fick's law and may be written as follows

$$i_{Lim} = \frac{zFD_{O2,T}c_B}{d} \tag{8}$$

where z = number of electrons transferred, F = Faraday's constant, $D_{O2,T}$ = oxygen transport function, c_B = oxygen concentration at the concrete surface and d = concrete cover thickness. To describe the oxygen transport in concrete an empirical expression proposed by Papadakis et al. (1991) is chosen

$$D_{O2} = 1.92 \cdot 10^{-6} \varepsilon_p \left(1 - RH\right)^{2.2} \tag{9}$$

where D_{O2} = oxygen transport function at reference temperature and ε_P = concrete porosity. The influence of the temperature on the oxygen transport is modeled with an Arrhenius equation

$$D_{O2,T} = D_{O2} \exp\left(\frac{\Delta U_{O2}}{RT}\right) \tag{10}$$

where ΔU_{O2} = activation energy for oxygen diffusion, R = universal gas constant and T = absolute temperature. Values for the activation energy of oxygen diffusion can be found e.g. in Page & Lambert (1987) and Isgor et al. (2009).

Furthermore, the concrete resistivity, which is affected by numerous factors, such as the moisture content, concrete microstructure, ion concentration, temperature and possible fiber content, plays an important role in determining the polarization of the steel surface in concrete. Values for concrete resistivity for various exposure conditions and different concrete moisture contents can be found in the literature, e.g. in Polder (2001). For simplicity it is assumed that the resistivity only depends on the moisture content and temperature in the present model. Experimental studies investigating the relation between moisture content and resistivity for different concrete and mortar types have been carried out and can be found e.g. in Hötte (2003).

To describe the moisture dependence of the concrete resistivity a power law is used in the present model

$$\rho = \sqrt[c]{\frac{\frac{1}{MC} - a}{b}} \tag{11}$$

where ρ = concrete resistivity at reference temperature, a,b,c = non-physical fitting parameters and MC = moisture content. Experimental data presented by Hötte (2003) and fitted data (Equation 11), for a CEM 1 concrete is given in Figure 2. The influence of temperature on the resistivity is modeled with an Arrhenius equation

$$\rho_T = \rho \exp\left(\frac{\Delta U_{RH}}{RT}\right) \tag{12}$$

where ρ_T = concrete resistivity and ΔU_{RH} = activation energy for moisture transport. Values for the activation energy of moisture transport can be found e.g. in Chrisp et al. (2001).

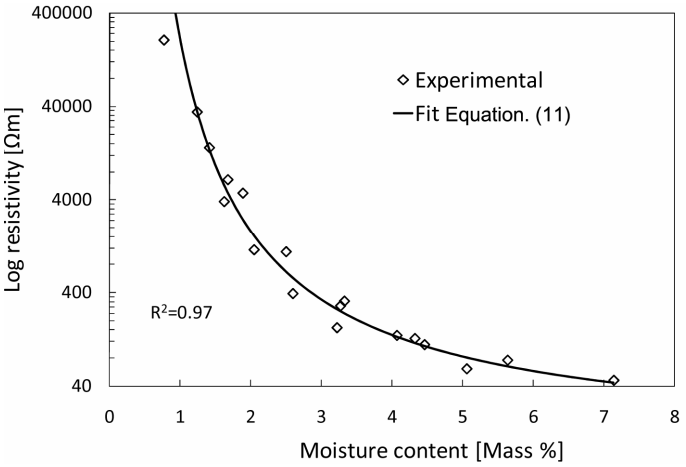

Figure 2. Experimental (Hötte (2003)) and fitted data for concrete resistivity as a function of moisture content.

2.2 *FEM based crack propagation model*

After the corrosion current density along the concrete steel interface is predicted by the corrosion model, deformations and crack propagation in the concrete cover due to the formation of expansive corrosion products can be determined using the proposed FEM based crack propagation model. The present fracture mechanics model assumes uniform corrosion along the reinforcement leading to a 2D problem in a plain strain formulation. The crack propagation in the concrete cover of reinforced concrete structures is modeled assuming that no corrosion products diffuse into concrete pores, voids or cracks.

In the proposed model two different fracture types are considered accounting for the crack propagation in the concrete cover due to corrosion. The underlying assumption of the proposed model for cracking in the concrete cover is Mode-I crack propagation. It is assumed that the crack propagates in the concrete cover when the tensile stresses due to expansion of the corrosion products exceed the tensile strength of the concrete. Debonding effects between concrete and reinforcement are described by Mixed-mode crack propagation. Both phenomena, cracking in the concrete cover and debonding, are described by a discrete cracking approach in the present model. Tension softening is described based on a cohesive discrete cracking model in which multilinear softening relations are adopted from Skoček & Stang (2009). The fracture energy of the Mode-1 crack opening behavior during the Mixed-mode crack propagation (debonding effects) is reduced by a factor of 10 compared to pure Mode-I crack propagation to account for a reduced bonding between concrete and corrosion products. A constant shear modulus of 10GPa after cracking is assumed for the Mixed-mode crack propagation.

Zero-thickness cohesive interface elements are implemented perpendicular (simulating Mode-I crack propagation in the concrete cover) and circumferential (simulating Mixed-mode crack propagation) to the reinforcement allowing crack propagation only in the implemented interface elements. However, comparing with experimental results of crack patterns due to expansion of corrosion products (see e.g. Andrade et al. (1993), Alonso et al. (1998), Val et al. (2009)) the definition of a prescribed crack path seems to be appropriate.

Linear elastic material properties are defined for the semi-infinite concrete body, corrosion layer and reinforcement section (see Fig. 3). Elastic material properties for the corrosion products can be found in the literature (see e.g. Molina et al. (1993), Suda et al. (1993), Caré et al. (2008)). For the present model material properties proposed by Ouglova et al. (2006) are used. A Young´s modulus of 2.1 GPa and a Poisson ratio of 0.2 are defined for the corrosion layer.

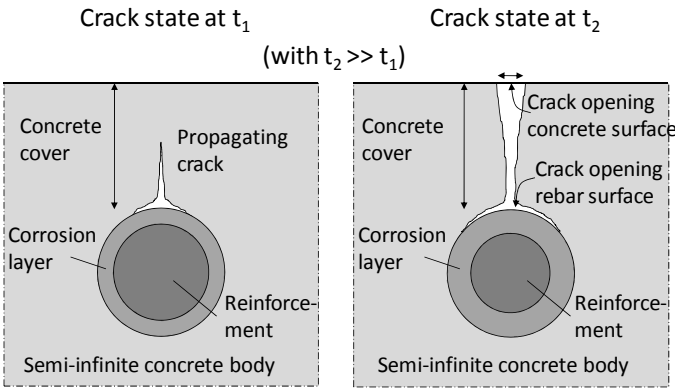

Figure 3. Crack propagation in proposed FEM model.

Since corrosion of reinforcement is not a typical load scenario in commercial FEM codes a special way of load application is used to model the propagation of cracks in the concrete cover. Initially, the cross sectional area of the reinforcement, reduced due to corrosion, is determined, and afterwards the expansion of the corroded reinforcement section is modeled. Crack propagation as well as load application in the FEM model and basic geometrical considerations are illustrated in Figure 3 and Figure 4, respectively. For the determination of the corroded reinforcement section Faraday´s law is used, which describes the relation between thickness reduction per time unit and corrosion current density, predicted by the FEM based corrosion model

$$X(t) = \frac{M}{zF\rho}\int_0^t i_{corr}(t)dt \tag{13}$$

where $X(t)$ = thickness reduction, $i_{corr}(t)$ = corrosion current density, M = mol mass of the metal, z = number of electrons in the reaction equation for the anodic reaction and ρ = density of the metal. For the present model 100% current efficiency is assumed meaning that all corrosion current is used for dissolution of iron.

Initially, the reinforcement with a radius R_O is embedded in the concrete.

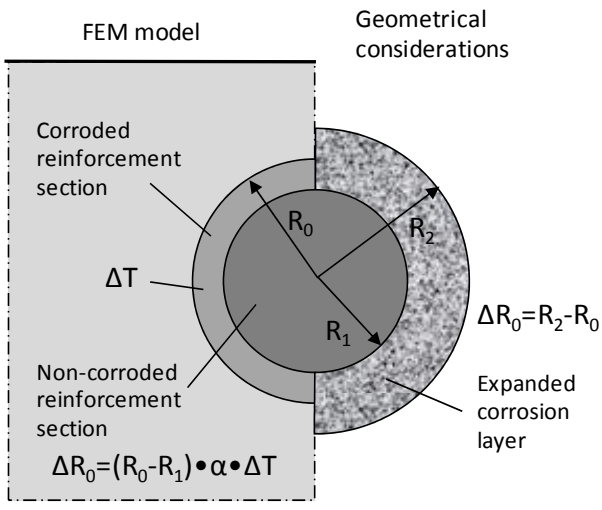

Figure 4. Load application in FEM model (left) and basic geometrical considerations (right) of crack propagation model.

Assuming uniform corrosion the cross sectional reduction of the reinforcement can be calculated

$$R_1 = R_0 - X \tag{14}$$

where R_1 = remaining radius of non-corroded reinforcement, R_0 = initial radius of reinforcement and X = thickness reduction according to Equation (13).

The linear expansion coefficient η can be written as follows

$$\eta = \frac{\Delta R_0}{X} \tag{15}$$

where ΔR_0 = increase of the initial radius of the reinforcement due to the expansion of corrosion products.

A thermal analogy is used to model the expansive nature of the corrosion products applying a thermal load to the corroded reinforcement section (see Fig. 4). Assuming a constant coefficient of thermal expansion, the applied temperature increment has to represent the formed corrosion product. Furthermore, the resulting thermal expansion has to be equal to the linear expansion coefficient in Equation 15. As mentioned before, the formation of uniformly distributed $Fe_2O_3 \cdot H_2O$ as corrosion product is assumed with a volume expansion coefficient of 6.3. Assuming isotropic material properties of the corrosion products, the linear expansion coefficient is one third of the volume expansion coefficient. Hence, the linear expansion coefficient applied to the corroded reinforcement section in proposed crack propagation model is 2.1 assuming the formation of $Fe_2O_3 \cdot H_2O$ as corrosion product.

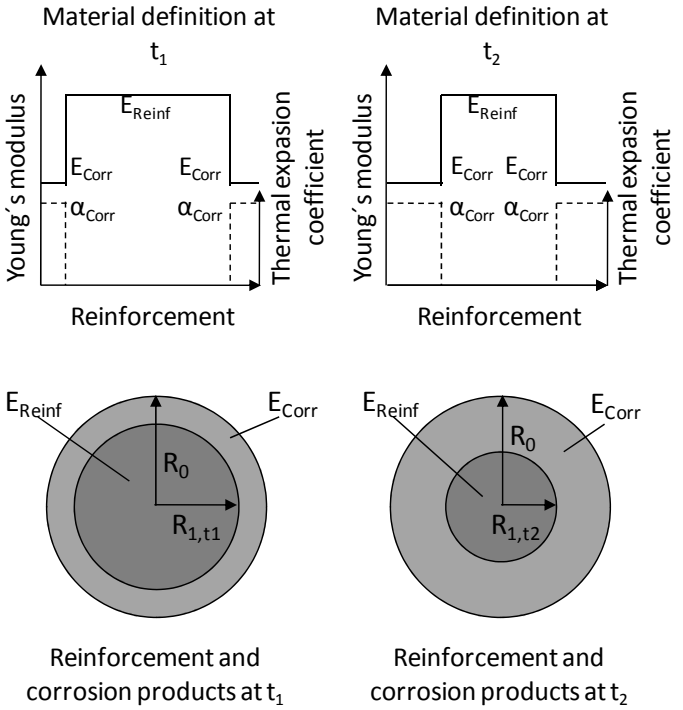

Figure 5. Time dependent material definitions for reinforcement and corrosion layer in crack propagation model.

Since the corroded reinforcement section increases over time (see Equation 13 and 14) the area which is subjected to the thermal load needs to be revaluated to obtain the correct stress state in the model. For each time step of the analysis the corresponding material properties have to be assigned to the correct domains in the finite element model. This is because the stress distribution and hence the crack propagation in the surrounding concrete depends on the interaction between the remaining reinforcement section, the corrosion layer and the elastic part of the semi-infinite concrete body. The time dependent material definitions and load application proposed for the present crack propagation model are given in Figure 5.

3 NUMERICAL EXAMPLE

To demonstrate the potential use of the proposed combined modeling approach a numerical example is given.

Initially, the corrosion model is used to predict the corrosion current density for various exposure conditions (varying moisture contents, temperature and oxygen). The model geometry for the numerical example is given in Figure 6. The polarization behavior of the reinforcement described by Equations (4) and (5) for the anodic and cathodic sites, respectively are illustrated in Figure 7. To reduce computational time the symmetrical properties of the system are utilized and only half of the geometry is modeled. The input parameters used in the analysis are given in Table 1. For the numerical solution of the time dependent corrosion problem, involving solution of Equations (1), (2) and (6), the commercial FEM software COMSOL Multiphysics is used. 5725 triangular elements are used to describe the concrete and steel domain, with a finer mesh in the anodic reinforcement region. Lagrange quadratic elements are used as element type and the time steps are chosen by the solver.

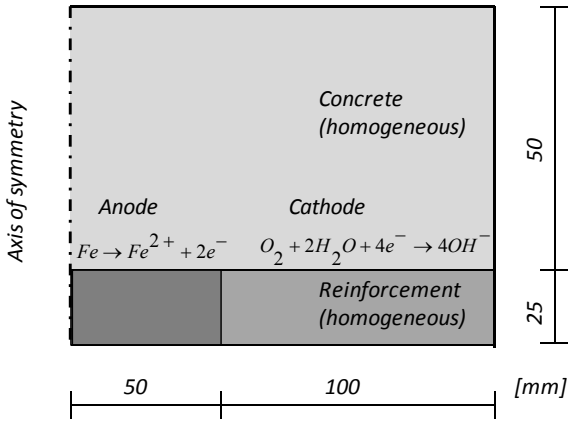

Figure 6. Corrosion model geometry for numerical example (not to scale).

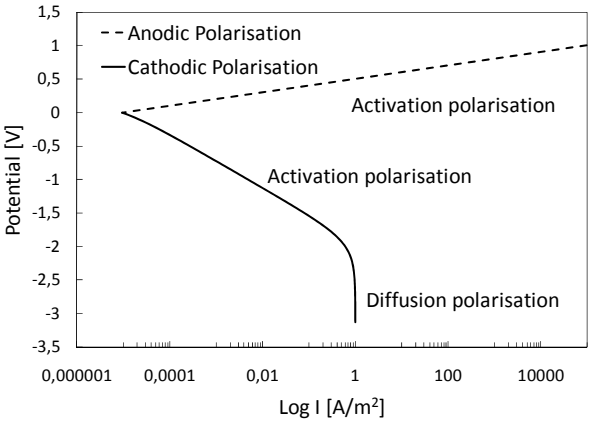

Figure 7. Corrosion model boundary conditions for numerical example.

Table 1. Input parameters (corrosion and crack propagation model) for numerical example.

Parameter	Value	Dimension
Anodic exchange current density at equilibrium	1.88 E-04	A/m^2
Anodic equilibrium potential	-0.78	V
Anodic Tafel constant	0.06	V/dec
Cathodic exchange current density at equilibrium	6.25 E-06	A/m^2
Cathodic equilibrium potential	0.16	V
Cathodic Tafel constant	0.16	V/dec
Concrete resistivity	Equation (11)	ohm m
Initial bulk humidity	0.9	-
Moisture transport	Equation (6) and (7)	m/s^2
Limiting current density	Equation (8)	A/m^2
Oxygen transport	Equation (6) and (9)	m/s^2
Temperature	Equation (6)	K
Concrete cover	50	mm
Reinforcement diameter	25	mm
Corroded reinforcement section	Equation (13)	mm
Young´s modulus reinforcement	210	GPa
Poisson ratio reinforcement	0.3	-
Young´s modulus concrete	30	GPa
Poisson ratio concrete	0.2	-
Tensile strength concrete	4	MPa
Young´s modulus corrosion products	2.1	GPa
Poisson ratio corrosion products	0.2	-
Thermal expansion coefficient corrosion products	2.1	-/K
Temperature increment	1	K

The FEM based crack propagation model is used to demonstrate the influence of varying corrosion rates, predicted by the corrosion model, on the propagation of corrosion induced cracks in the concrete cover of reinforced concrete structures. The model geometry chosen for the numerical example is illustrated in Figure 8. A model size of 225mm proved to be sufficient to represent the semi-infinite concrete body, which was checked before actual simulations were carried out with the crack propagation model. The implemented cohesive relations for the interface elements perpendicular and circumferential to the reinforcement are given in Figure 9. Input parameters used in the example are given in Table 1. To simulate the crack propagation due to the expansive nature of corrosion products the commercial FEM software DIANA is used. 902 quadrangular elements (2864 DOF´s) are used to describe the interface, concrete, reinforcement and corrosion layer domain in the model. Nonlinear solution is obtained using a standard Newton-Raphson method with a displacement controlled convergence criterion.

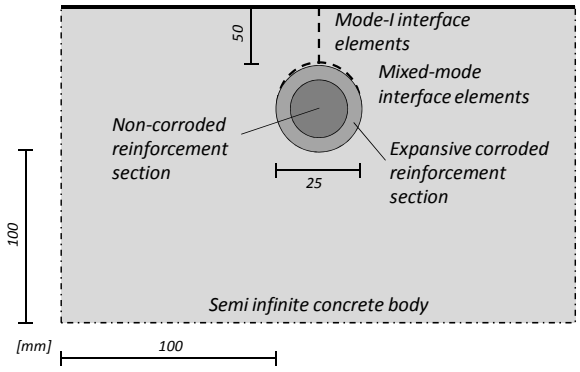

Figure 8. Crack propagation model geometry for numerical example (not to scale).

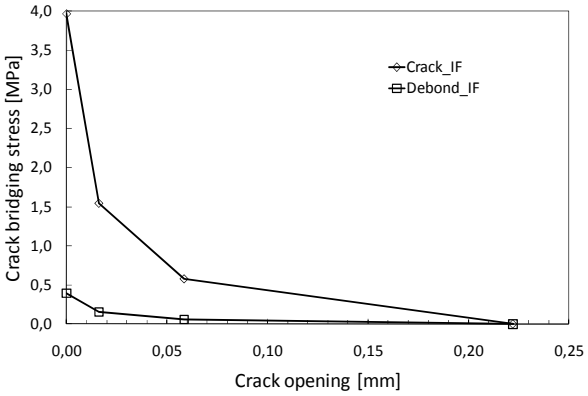

Figure 9. Cohesive relation for Mode-I and Mixed-mode interface elements in numerical example after Skoček & Stang (2009).

4 RESULTS

Results of the numerical example are presented in Figures 10-12. Initially, the FEM based corrosion model was used to predict corrosion current densities for varying exposure conditions. Afterwards, the proposed crack model was used to relate the predicted corrosion current densities and model the propagation of cracks in the surrounding concrete due to formation of expansive corrosion products.

4.1 *Corrosion model*

To demonstrate the potential use of the corrosion model, corrosion current densities were predicted

with the model for three different exposure scenarios. For the presented numerical example the effects of varying relative humidity, temperature and oxygen content on the corrosion current density were studied. More details on the three exposure scenarios are given in Table 2. Results of the numerical simulation are given in Figure 10. It is evident from the results that the corrosion current density depends on the investigated exposure scenarios. The most pronounced effect can be observed for exposure scenario 1, following the changing moisture content in the concrete due to the applied boundary conditions and moisture transport function. The impact of exposure scenarios 2 and 3 appears to be less distinct for the investigated geometry and boundary conditions.

Table 2. Parameters describing different exposure scenarios.

Scenario	Relative humidity [-]	Temperature [K]	Oxygen [mol/m^3]
1	0.72 - 0.91	295	1
2	0.8	275 - 295	1
3	0.8	295	0.2 - 1

4.2 *Crack propagation model*

Crack openings for different locations in the surrounding concrete as a function of the corrosion layer thickness are given in Figure 11. As expected, the crack opens first at the rebar surface due to the expansion of the corrosion layer and is propagating towards the concrete surface. As soon as the crack reaches the concrete surface a linear relation between thickness of corrosion layer and crack opening can be observed. Figure 12 illustrates the crack opening at the concrete surface as a function of time for the predicted corrosion current densities. It is evident from the results that crack opening as well as propagation depend on the corrosion current density predicted by the corrosion model. For the presented numerical example it can be seen, that the crack opening as well as the crack propagation are delayed for the corrosion current densities determined for the exposure scenarios 2 and 3 compared to exposure scenario 1.

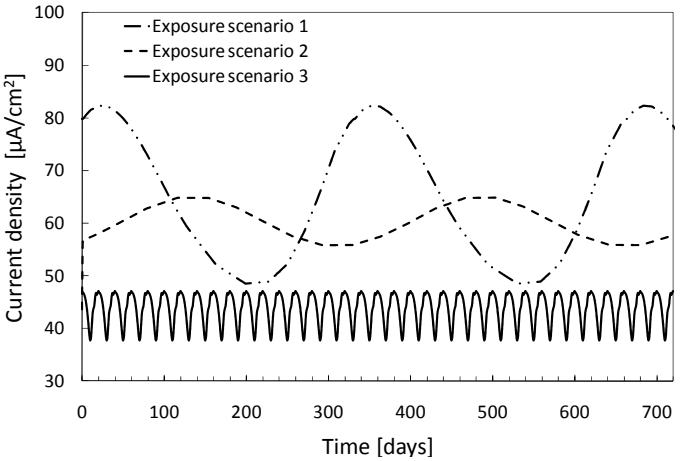

Figure 10. Corrosion current densities for exposure scenarios.

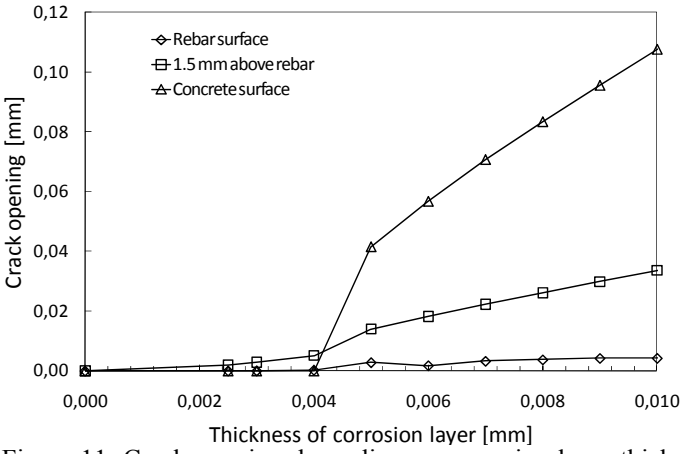

Figure 11. Crack opening depending on corrosion layer thickness for model geometry and cohesive relation.

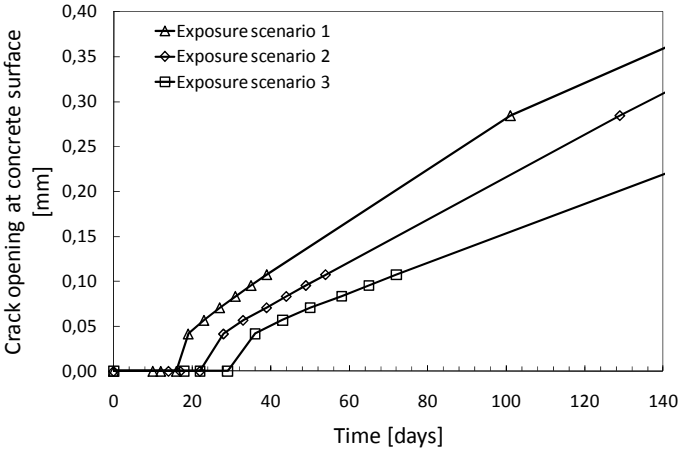

Figure 12. Crack opening at concrete surface for predicted corrosion current densities.

5 SUMMARY AND CONCLUSIONS

A combined electrochemical and mechanical modeling approach to simulate the formation of cracks in reinforced concrete structures due to corrosion was presented. A two-phase finite element based corrosion model was used to determine the corrosion current density of steel in concrete taking into account the impact of varying exposure conditions. A crack propagation model was used to simulate the formation of cracks in the concrete cover due to the expansive nature of formed corrosion products. The proposed crack propagation model does not take into account the diffusion of corrosion products into concrete pores, voids or cracks, resulting in an overestimation of the crack propagation. Furthermore, the presented modeling approach does not take the influence of corrosion induced cracks on the transport properties of the concrete into account.

To demonstrate the potential use of the proposed combined modeling approach a numerical example was presented. In the example the influence of various parameters of the corrosion model on the crack propagation were investigated. The presented results illustrate the major impact of the corrosion current density on the crack propagation. Furthermore, the

need for a realistic prediction of the corrosion rate as well as selection of the corrosion products formed to simulate formation of corrosion induced concrete cover cracking is evident from the presented results.

For a better understanding of the corrosion process in concrete structures as well as subsequent formation of cracks, future investigations should also focus on the impact of concrete material parameters, model geometry as well as mechanical properties of the corrosion products formed (see e. g. Solgaard et al. (2009)).

ACKNOWLEDGMENTS

The first author gratefully acknowledges the financial support of Femern Bælt A/S, Sund & Belt Holding A/S and The Danish Agency for Science, Technology and Innovation.

REFERENCES

Alonso, C., Andrade, C., Rodriguez, J., & Diez, J. M. 1998. Factors controlling cracking of concrete affected by reinforcement corrosion. *Materials and Structures* 31: 435-441.

Andrade, C., Alonso, C., & Molina, F. J. 1993. Cover cracking as a function of bar corrosion: Part 1 - Experimental test. *Materials and Structures* 26: 453-464.

Bardal, E. 2004. Corrosion and Protection. *Engineering Materials and Processes*. London, UK: Springer, 1st edition.

Bazant, Z. P. 1979. Physical model for steel corrosion in concrete sea structures - Application. *Journal of the Structural Division* 105: 1155–1166.

Bazant, Z., Xi, Y., Molina, L. & Jennings, H. M. 1994. Moisture Diffusion in Cementitious Materials - Moisture Capacity and Diffusivity. *Advanced Cement Based Materials* 1: 258-266.

Caré, S., Nguyen, Q. T., L´Hostis, V. & Berthaud, B. 2008. Mechanical properties of the rust layer induced by impressed current method in reinforced mortar. *Cement and Concrete Research* 38: 1079-1091.

Chernin, L., Val, V. D. & Volokh K. Y. 2009. Analytical modelling of concrete cover cracking by corrosion of reinforcement. *Materials and Structures published online*.

Chrisp, T. M., Starrs, G., McCarter, W. J., Rouchotas, E. & Blewett, J. 2001. Temperature - conductivity relationships for concrete: An activation energy approach. *Journal of Material Science Letters* 20: 1085-1087.

Hötte, C. 2003. Bestimmung des Feuchtezustandes von Mauerwerk mit Hilfe von Multiring-Elektroden - Untersuchungen zum Ankoppelungsmörtel und an Probewänden. *Diplomarbeit* Technische Hochschule Aachen, Institut für Bauforschung.

Isgor, B. O. & Razaqpur, G. A. 2006. Modelling steel corrosion in concrete structures. *Materials and Structures* 39: 291–302.

Isgor, O. B., Pour-Ghaz, M. & Ghods, P. 2009. The effect of temperature on the corrosion of steel in concrete. Part 2: Model verification and parametric study. *Corrosion Science* 51: 426-433.

Künzel, H. M. 1994. Verfahren zur ein- und zweidimensionalen Berechnung des gekoppelten Wärme- und Feuchtetransports in Bauteilen mit einfachen Kennwerten. *PhD Thesis* Universität Stuttgart.

Küter, A. 2009. Management of reinforcement corrosion - A thermodynamical approach. *PhD Thesis* Department of Civil Engineering, Technical University of Denmark.

Li, V. 2004. A New Research Framework for Sustainable Infrastructures. *Seminar* Department of Civil Engineering, Technical University of Denmark.

Liu, Y. & Weyers, R. E. 1998. Modeling the time-to-corrosion cracking in chloride contaminated reinforced concrete structures. *ACI Materials Journal* 95: 675-681.

Marcotte, T. D. & Hansson, C. M. 2007. Corrosion products that form on steel within cement paste. *Materials and Structures* 40: 325-340.

Molina, F. J., Alonso, C., & Andrade, C. 1993. Cover cracking as a function of rebar corrosion: part 2 - numerical model. *Materials and Structures* 26: 532–548.

Noghabai, K. 1999. FE-Modelling of cover splitting due to corrosion by use of inner softening band. *Materials and Structures* 32: 486-491.

Ouglova, A. Berthaud, Y. Francois, M. & Foct, F. 2006. Mechanical properties of an iron oxide formed by corrosion in reinforced concrete structures. *Corrosion Science* 48: 3988-4000.

Page, C. L. & Lambert, P. 1987. Kinetics of oxygen diffusion in hardened cement pastes. *Journal of Material Science* 22: 942-946.

Papadakis, V. G., Vayenas, C. G. & Fardis, M. N. 1991. Physical and Chemical Characteristics Affecting the Durability of Concrete. *ACI Materials Journal* 8: 186-196.

Pel, L. 1995. Moisture transport in building materials. *PhD Thesis* Eindhoven University of Technology.

Polder, R. B. 2001. Test methods for onsite measurement of resistivity of concrete - a RILEM TC-154 technical recommendation. *Construction and building materials* 15: 125-131.

Rendell, F., Jauberthie, R. & Grantham, M. 2002. Deteriorated Concrete - Inspection and physicochemical analysis. London, UK: Thomas Telford, 1st edition.

Scheffler, G. A. 2009. Validation of hygrothermal material modelling under consideration of the hysteresis of moisture storage. *PhD Thesis* Technische Universität Dresden.

Skoček, J. & Stang, H. 2009. Upscaling of fracture properties - discrete modeling. *Submitted to Cement and Concrete Research*.

Solgaard, A. O. S., Michel, A., Stang, H., Geiker, M. R., Edwardsen, C. & Küter, A. 2009. Numerical modeling of cracking of concrete due to corrosion of reinforcement - Impact of cover thickness and concrete toughness. *FraMCos-7 - 7th International Conference on Fracture Mechanics of Concrete and Concrete Structures; Conference proceedings. Jeju, Korea, 23-28 May 2010.*

Stern, M. & Geary, A. L. 1957. Electrochemical polarization I. A theoretical analysis of the shape of polarization curves. *Journal of the Electrochemical Society* 104: 56–63.

Suda, K., Misra, S. & Motohashi, K. 1993. Corrosion products of reinforcing bars embedded in concrete. *Corrosion Science* 35: 1543-1549.

Val, D. V., Chernin, L. & Stewart, M. G. 2009. Experimental and numerical investigation of corrosion-induced cover cracking in reinforced concrete structures. *Journal of Structural Engineering* 135: 376-385.

Warkus, J., Raupach, M. & Gulikers, J. 2006. Numerical modeling of corrosion - Theoretical backgrounds -. *Materials and Corrosion* 57: 614-617.

Wittmann, F. H. 1992. Feuchtigkeitstransport und Dauerhaftigkeit von Beton. *Wissenschaftlich Technische Arbeitsgemeinschaft für Bauwerkserhaltung und Denkmalpflege*.